

# MEDIC: ZERO-SHOT MUSIC EDITING WITH DISENTANGLED INVERSION CONTROL

**Anonymous authors**

Paper under double-blind review

## ABSTRACT

Text-guided diffusion models make a paradigm shift in audio generation, facilitating the adaptability of source audio to conform to specific textual prompts. Recent works introduce inversion techniques, like DDIM inversion, to zero-shot editing, exploiting pretrained diffusion models for audio modification. Nonetheless, our investigation exposes that DDIM inversion suffers from an accumulation of errors across each diffusion step, undermining its efficacy. Moreover, existing editing methods fail to achieve effective complex non-rigid music editing while maintaining essential content preservation and high editing fidelity. To counteract these issues, we introduce the *Disentangled Inversion* technique to disentangle the diffusion process into triple branches, rectifying the deviated path of the source branch caused by DDIM inversion. In addition, we propose the *Harmonized Attention Control* framework, which unifies the mutual self-attention control and cross-attention control with an intermediate Harmonic Branch to progressively achieve the desired harmonic and melodic information in the target music. Collectively, these innovations comprise the *Disentangled Inversion Control (DIC)* framework, enabling accurate music editing while safeguarding content integrity. To benchmark audio editing efficacy, we introduce *ZoME-Bench*, a comprehensive music editing benchmark hosting 1,100 samples spread across ten distinct editing categories. This facilitates both zero-shot and instruction-based music editing tasks. Our method achieves unparalleled performance in edit fidelity and essential content preservation, outperforming contemporary state-of-the-art inversion techniques.<sup>1</sup> Both code and benchmark will be released.

## 1 INTRODUCTION

Text-guided diffusion models (Song et al., 2020; Song & Ermon, 2020; Peebles & Xie, 2023) have made great progress in audio generation (Evans et al., 2024a;b), leveraging their impressive capability for realistic and varied outputs. In particular, these models (Liu et al., 2023b; Huang et al., 2023; Liu et al., 2024) provide the foundation for prompt-based audio editing, offering new opportunities to modify audio landscapes for specific *textual prompts*. Early audio editing strategies rely on training models from scratch (Copet et al., 2023; Agostinelli et al., 2023) or test-time optimization (Paissan et al., 2023; Plitsis et al., 2024), hampered by intensive computational demands. Recent works (Manor & Michaeli, 2024; Zhang et al., 2024) in zero-shot audio editing have been made through Denoising Diffusion Implicit Models (DDIM) (Song et al., 2020) and Denoising Diffusion Probabilistic Models (DDPM) (Ho et al., 2020) inversion techniques, but challenges remain.

Key among these challenges are maintaining *fidelity of editing* - ensuring the editing aligns with the provided instructions - and *essential content preservation*, ensuring that the unaltered musical attributes in the target prompts remain unchanged. However, balancing these objectives involves a careful exchange of information between the source and target branch in diffusion processes, with existing inversion methods like DDIM proving sub-optimal for conditional diffusion models (Mokady et al., 2023). Enhanced versions of edit-friendly DDPM inversion (Huberman-Spiegelglas et al., 2024) make strides in preservation by imprinting the source onto the noise space. However, this comes at the expense of reduced modification capabilities due to noise reduction.

<sup>1</sup>Audio samples are available at <https://MEDIC-Zero.github.io/>.

054 In this work, we rigorously examine the shortcomings of the DDIM inversion approach. Our  
 055 comprehensive analysis indicates that while techniques like DDIM inversion provide an editable  
 056 foundation for audio synthesis, they lack precision and may compromise the integrity of the original  
 057 audio. The primary issue stems from the assumption of perfect reversibility in the ordinary differential  
 058 equation (ODE) process, which is frequently not met during text-conditional editing. Consequently,  
 059 this leads to distortions during the inversion. And the implementation of Classifier-free Guidance  
 060 (CFG) (Ho & Salimans, 2021) aims to improve text adherence. However, it inadvertently amplifies the  
 061 accumulated errors from the inversion process. Moreover, attention control (Cao et al., 2023; Hertz  
 062 et al., 2022) has shown promise in achieving high fidelity and essential content preservation. For  
 063 instance, MusicMagus (Zhang et al., 2024) introduces Cross-Attention Control for fine-grained music  
 064 manipulation of rigid tasks. Nevertheless, these methods fail to resolve the issues of accumulated  
 065 errors and struggle to achieve accurate editing for both rigid and non-rigid tasks, as illustrated in  
 066 Figure 1. We introduce an innovative *Disentangled Inversion Control* technique to bridge this gap.  
 067 This technique has two main components: *Harmonic Attention Control* and *Disentangled Inversion*.  
 068 Cross-attention control (Hertz et al., 2022) and mutual self-attention control (Cao et al., 2023) have  
 069 demonstrated robust editing capabilities for rigid and non-rigid image editing tasks, respectively.  
 070 However, blindly combining these two approaches sequentially for music editing can result in sub-  
 071 optimal outcomes, particularly in the original dual-branch setup, where it struggles with global  
 072 attention refinement. To address this challenge, we introduce an intermediate branch called the  
 073 Harmonic Branch, designed to modify both rigid and non-rigid attributes in music progressively.  
 074 Furthermore, we disentangle the diffusion process into triple branches, correcting the deviation path  
 075 caused by CFG in the source branch, which affects the essential content preservation. The other  
 branches remain unchanged to ensure the highest possible edit fidelity.

076 Due to a lack of standardized benchmarks in audio editing, we introduce ZoME-Bench. The  
 077 first music editing benchmark consists of 1,100 audio clips, distributing them into 10 rigorously  
 078 curated editing categories across rigid and non-rigid tasks. Each entry is carefully assembled,  
 079 comprising a source prompt, a target prompt, human instruction, and blended words intended  
 080 for editing. Experimental results on ZoME-Bench indicate that MEDIC outperforms baselines,  
 081 achieving significant improvements in essential content preservation and editing fidelity. Additionally,  
 082 MEDIC demonstrates state-of-the-art performance in the variable-length music editing settings of the  
 083 MusicDelta dataset.

084 Our contributions can be summarized as follows. 1) We introduce a novel, training-free methodology  
 085 called Disentangled Inversion Control (DIC), designed to facilitate consistent manipulations of musi-  
 086 cal elements and intricate non-rigid editing tasks. 2) An *Harmonized Attention Control* framework is  
 087 introduced to unify cross-attention and mutual self-attention control, which enables both rigid and  
 088 non-rigid editing. 3) We present *Disentangled Inversion Technique* to achieve superior results with  
 089 negligible inversion error by branch disentanglement and correction, aiding in accurately editing the  
 090 music while preserving the content information. 4) We build a new benchmark for music editing,  
 091 named *ZoME-Bench*, which supports both zero-shot and instruction-based music editing.

## 092 2 RELATED WORKS

093 **Text-based Audio editing.** The objective of text-based audio editing (Paissan et al., 2023; Plitsis  
 094 et al., 2024; Han et al., 2023a) is to utilize diffusion models to manipulate audio content based  
 095 on the provided target prompt. Existing methodologies for addressing these intricate challenges  
 096 typically follow one of three paths. The first involves attempts to develop end-to-end editing  
 097 models (Copet et al., 2023; Agostinelli et al., 2023; Chen et al., 2024) that employ diffusion processes.  
 098 However, these efforts are often hampered by indirect training strategies or a lack of comprehensive  
 099 datasets. The second path involves test-time optimization strategies that utilize large pre-trained  
 100 models for editing (Paissan et al., 2023; Plitsis et al., 2024). Despite their versatility, these methods  
 101 are often burdened by the significant computational demands of fine-tuning diffusion models or  
 102 optimizing text-embeddings for signal reconstruction. Some methods may choose to employ both  
 103 strategies (Kawar et al., 2023), further increasing the computational load. The final path involves  
 104 inversion techniques, which typically use DDPM (Huberman-Spiegelglas et al., 2024; Wu & De la  
 105 Torre, 2023)/DDIM (Song et al., 2020; Zhang et al., 2024) inversion strategies to extract diffusion  
 106 noise vectors that match the source signal. Given its rapid and intuitive zero-shot editing capabilities,  
 107 we have chosen inversion techniques as our primary research framework. In this work, we propose

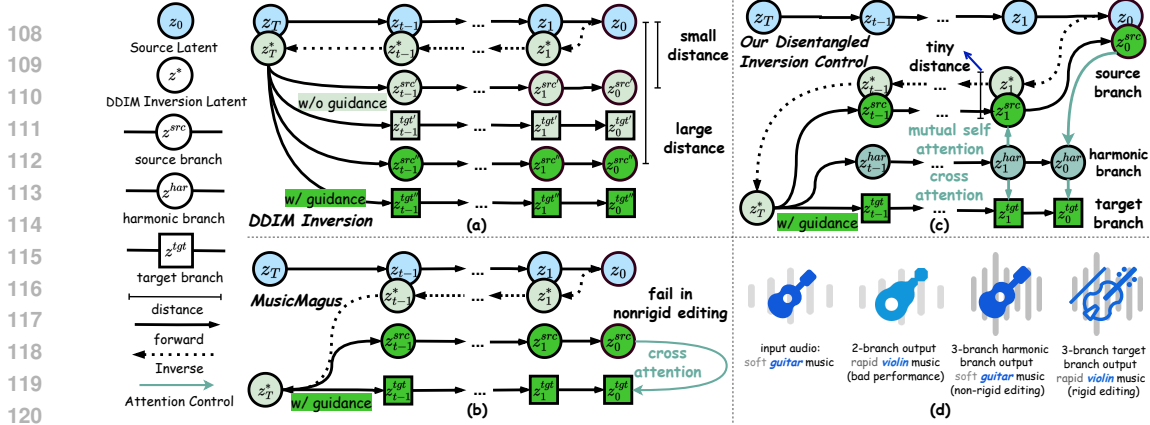


Figure 1: Comparisons of our method with two-branch inversion techniques, including DDIM Inversion and MusicMagus. (a) Framework of DDIM Inversion, showing configurations with and without classifier-free guidance. (b) Framework of MusicMagus, which incorporates cross-attention control. (c) Framework of our method, featuring disentangled inversion control. (d) An illustration comparing the output of the two-branch techniques with the progressive output of our triple-branch approach.

a new inversion technique named Disentangled Inversion Control. This technique aims to achieve accurate editing while preserving structural information.

**Inversion Techniques.** The field of image inversion techniques has experienced significant progress in recent years (Brooks et al., 2023; Kim et al., 2022; Parmar et al., 2023; Dhariwal & Nichol, 2021). While the DDIM inversion proves effective for unconditional diffusion models (Song et al., 2020; Wallace et al., 2023), its limitations become apparent when applied to text-guided diffusion models, particularly when classifier-free guidance is necessary for meaningful editing. A range of solutions (Mokady et al., 2023; Tumanyan et al., 2022) have been proposed to address these challenges. For example, Negative-Prompt Inversion strategically assigns conditioned text embeddings to Null-Text embeddings, effectively reducing potential deviation during editing. Conversely, Edit Friendly DDPM provides an alternative latent noise space via modified DDPM sample distributions, promoting the successful reconstruction of the desired image (Huberman-Spiegelglas et al., 2024). Optimization-based inversion methods using specific latent variables have recently gained popularity (Ju et al., 2023; Kawar et al., 2023). These are designed to minimize accumulated errors stemming from the DDIM inversion. Techniques such as Null-Text Inversion (Mokady et al., 2023) are promising, but they introduce complexity and instability into the optimization process, making it relatively time-consuming. Differently, we introduce a plug-in-plus method called Disentangled Inversion Control to separate branches, achieving superior performance with considerably fewer computational resources.

### 3 DISENTANGLED INVERSION CONTROL

#### 3.1 PROBLEM DEFINITION AND BENCHMARK CONSTRUCTION

Despite significant work in text-to-audio generation models, particularly with the emergence of latent diffusion models (LDM), research on zero-shot music editing remains limited. Zero-shot music editing seeks to leverage the capabilities of text-to-music generation models to synthesize the desired music, denoted as  $x_0^{tgt}$ . This synthesized music should align with the target edited text prompt  $\mathcal{P}^*$ , which is directly modified from the source music  $x_0^{src}$  and its corresponding text prompt  $\mathcal{P}$ . We compress source audio signals into latent  $z_0^{src}$  for inversion.

To systematically validate our proposed method as a plug-and-play strategy for editing models, compare our method with existing zero-shot music editing methods, and compensate for the absence of standardized performance criteria for inversion and editing techniques, we construct a benchmark dataset named ZoME-Bench (Zero-shot Music Editing Benchmark). ZoME-Bench comprises 1,100 audio samples which are selected from MusicCaps (Doh et al., 2023), spanning ten different editing

types that include both rigid and non-rigid modifications. Each sample is accompanied by its corresponding source prompt, target prompt, human instruction, and source audio.

Additionally, we include annotations relevant to attention control, such as blended words, to facilitate detailed evaluations. Further details about our benchmark can be found in Appendix B.

### 3.2 MOTIVATION

Figure 1 and Preliminaries in Appendix A reveal that while techniques like DDIM inversion offer an editable base, they fall short of precision. This potentially compromising the essential content preservation. The implementation of Classifier-free Guidance (CFG) further amplifies the accumulated errors.

In the landscape of prompt-based editing (Dong et al., 2023; Kim et al., 2022; Feng et al., 2023), the ability to grasp the subtleties of linguistics and enable more granular cross-modal interactions stands as a formidable challenge. Hertz et al. (2022) acknowledges that in image editing, the fusion between text and visual modalities happens within the parameterized noise prediction network  $\epsilon_\theta$ . This leads to the development of various attention control techniques that guide the target denoiser network  $\hat{\epsilon}_\theta$  in the image domain to better align with target prompts. Yet, analogous control mechanisms for non-rigid music editing are noticeably limited.

Taking these insights forward, we introduce Disentangled Inversion Control (DIC), a novel approach to achieve both rigid and non-rigid music editing. DIC strategically disentangles the diffusion process as triple branches, allowing each branch to optimize its functionality. At the same time, the strategy leverages harmonized attention control to facilitate targeted editing, thus aligning with the dual objectives of preserving the original audio essence and ensuring edit relevance. We will first introduce *Harmonized Attention Control* in Section 3.3 and discuss *Disentangled Inversion* in Section 3.4.

### 3.3 HARMONIZED ATTENTION CONTROL FRAMEWORK

The denoising architecture denoted as  $\epsilon_\theta$ , is structured as a sequence of fundamental blocks, each comprising a residual block (He et al., 2015) followed by self-attention and cross-attention modules (Vaswani et al., 2023; Dosovitskiy et al., 2020; Liu et al., 2023c). At the denoising step  $t$ , the output of the  $(l - 1)$ -th block is passed through self-attention and then aligned with textual cues from prompt  $P$  within the cross-attention layer. The attention mechanism is formalized as:

$$\text{Attention}(Q, K, V) = MV = \text{Softmax}\left(\frac{QK^T}{\sqrt{d}}\right)V \quad (1)$$

where  $Q$  denotes the query features derived from the audio features,  $K$  and  $V$  represent the key and value features, and  $M$  is the attention map. We explore varying semantic transformations of audio content through harmonized attention control strategies — cross-attention control for rigid changes and mutual self-attention control for non-rigid adjustments. Finally, we introduce an intermediate branch to host the desired harmonic and melodic information in the target music. The framework of harmonized attention control is depicted in Figure 2.

#### 3.3.1 CROSS-ATTENTION CONTROL

Cross-attention Control (CAC) aims to inject the attention maps that are obtained from the generation with the original prompt  $\mathcal{P}$ , into a second generation with the target prompt  $\mathcal{P}^*$ . We follow the practice of Prompt-to-Prompt (Hertz et al., 2022) and define CAC as *Global Attention Refinement* and *Local Attention Blend*.

**Global Attention Refinement** At a given time step  $t$ , the attention map  $M_t$  for both the origin and target branches is computed, averaging over all layers with respect to the noised latent  $\mathbf{z}_t$ . We employ an alignment function  $A$  that maps each token index from the target prompt  $\mathcal{P}^*$  to its equivalent in  $\mathcal{P}$  or to None for non-aligning tokens. The refinement action is thus:

$$\text{Refine}(M_t^{src}, M_t^{tgt}, t) = \begin{cases} (M_t^{tgt})_{i,j} & \text{if } A(j) = \text{None}, \\ (M_t)_{i,j} & \text{otherwise.} \end{cases} \quad (2)$$

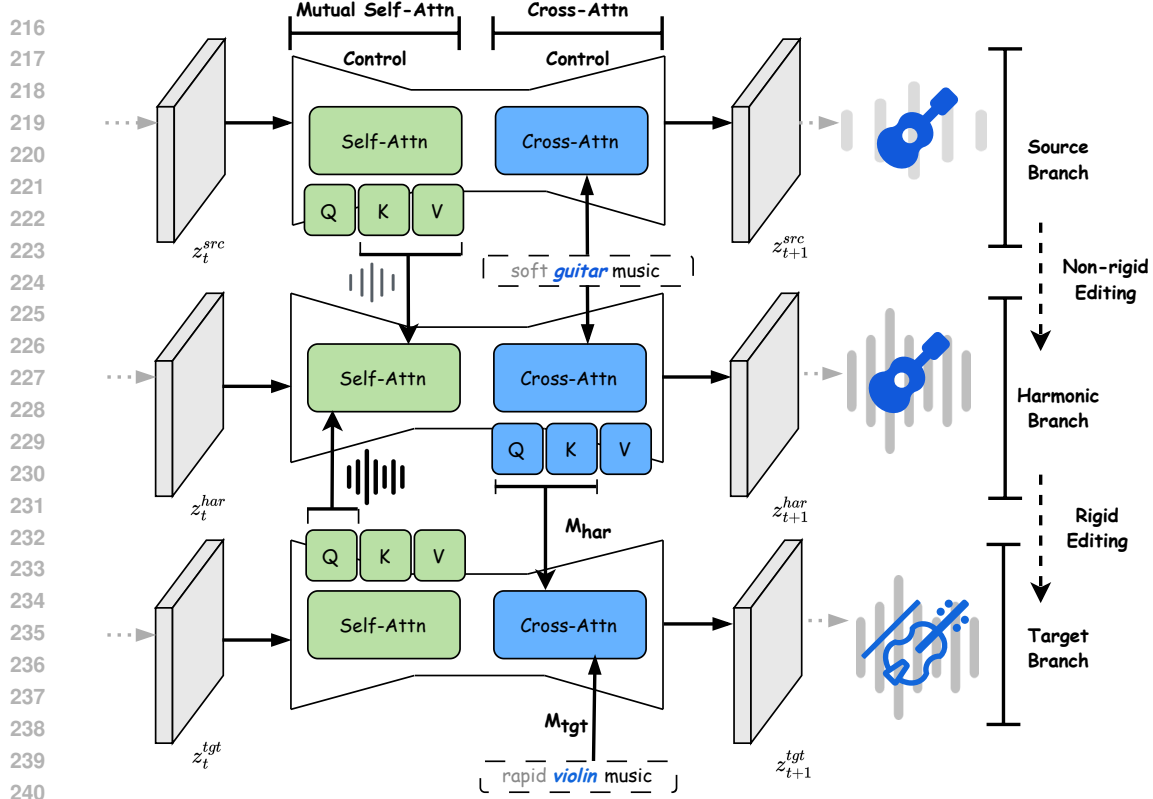


Figure 2: The framework of Harmonized Attention Control (HAC). HAC unifies cross-attention control and mutual self-attention control with an additional branch named *Harmonic Branch* to host the desired composition and structural information in the target music.

**Local Attention Blends** Beyond global attention, we incorporate a blending mechanism as suggested by Hertz et al. (2022) and Mokady et al. (2023). This method selectively integrates and maintains certain semantics by using target blend words  $w^{tgt}$  for semantic additions and source blend words  $w^{src}$  for semantic preservation. At each denoising step  $t$ , the mechanism operates on the target latent  $z_t^{tgt}$  as follows:

$$m_{tgt} = \text{Threshold} [M_t^{tgt}, w_{tgt}, k_{tgt}], \quad (3)$$

$$m_{src} = \text{Threshold} [M_t^{src}, w_{src}, k_{src}], \quad (4)$$

$$z_t^{tgt} = (1 - m^{tgt} + m^{src}) \odot z_t^{src} + (m^{tgt} - m^{src}) \odot z_t^{tgt} \quad (5)$$

where  $m_{tgt}$  and  $m_{src}$  are binary masks and threshold function is as delineated below:

$$\text{Threshold}(M, k) = \begin{cases} 1 & \text{if } M_{i,j} \geq k, \\ 0 & \text{if } M_{i,j} < k. \end{cases} \quad (6)$$

For simplicity, we define the process of local editing in Equation 5 as:

$$z_t^{tgt} = \text{LocalEdit}(z_t^{src}, z_t^{tgt}, M_t^{src}, M_t^{tgt}, w_{src}, w_{tgt}) \quad (7)$$

**Scheduling Cross-Attention Control** Applying cross-attention control only at early stages ensures creative flexibility while maintaining structure. Acting on insights from Hertz et al. (2022), we limit cross-attention to the initial phases up to a cutoff point  $\tau_c$ . This moderation allows us to capture the nuances and intended changes in musical compositions effectively. The approach is defined as:

$$\text{CrossEdit}(M^{src}, M^{tgt}, t) = \begin{cases} \text{Refine}(M_t^{src}, M_t^{tgt}) & \text{if } t \geq \tau_c, \\ M_t^{tgt} & \text{if } t < \tau_c. \end{cases} \quad (8)$$

**Algorithm 1** Harmonized Attention Control in one DDIM Forward Process

- 
- 1: **Input:** A source prompt  $\mathcal{P}$ , a target prompt  $\mathcal{P}^*$ , a source audio latent  $z_0$ , denoising network  $\epsilon_\theta(\cdot, \cdot, \cdot)$ , current time step  $\tau$ , source and target blend words  $w_{\text{src}}, w_{\text{tgt}}$ , input latents  $z_\tau^{\text{src}}, z_\tau^{\text{tgt}}, z_\tau^{\text{har}}$ .
  - 2:  $\epsilon_{\text{src}}, \{Q^{\text{src}}, K^{\text{src}}, V^{\text{src}}\}, M_{\text{src}} = \epsilon_\theta(z_\tau^{\text{src}}, \tau, c_{\text{src}})$
  - 3:  $\epsilon_{\text{tgt}}, \{Q^{\text{tgt}}, K^{\text{tgt}}, V^{\text{tgt}}\}, M_{\text{tgt}} = \epsilon_\theta(z_\tau^{\text{tgt}}, \tau, c_{\text{tgt}})$
  - 4:  $\{Q^{\text{har}}, K^{\text{har}}, V^{\text{har}}\} = \text{SelfEdit}(\{Q^{\text{src}}, K^{\text{src}}, V^{\text{src}}\}, \{Q^{\text{tgt}}, K^{\text{tgt}}, V^{\text{tgt}}\}, \tau)$
  - 5:  $\epsilon_{\text{har}}, M_{\text{har}} = \epsilon_\theta(z_\tau^{\text{har}}, \tau, c_{\text{src}}; \{Q^{\text{har}}, K^{\text{har}}, V^{\text{har}}\})$
  - 6:  $\hat{M}^{\text{tgt}} = \text{CrossEdit}(M_{\text{har}}, M_{\text{tgt}}, \tau)$
  - 7:  $\hat{\epsilon}_{\text{tgt}} = \epsilon_\theta(z_\tau^{\text{tgt}}, \tau, c_{\text{tgt}}; \hat{M}^{\text{tgt}})$
  - 8:  $z_{\tau-1}^{\text{src}}, z_{\tau-1}^{\text{tgt}}, z_{\tau-1}^{\text{har}} = \text{Sample}([z_\tau^{\text{src}}, z_\tau^{\text{tgt}}, z_\tau^{\text{har}}], [\epsilon_{\text{src}}, \hat{\epsilon}_{\text{tgt}}, \epsilon_{\text{har}}], \tau)$
  - 9:  $z_{\tau-1}^{\text{tgt}} = \text{LocalEdit}(z_{\tau-1}^{\text{src}}, z_{\tau-1}^{\text{tgt}}, M_{\tau-1}^{\text{src}}, M_{\tau-1}^{\text{tgt}}, w_{\text{src}}, w_{\text{tgt}})$
  - 10: **Output:**  $z_{\tau-1}^{\text{src}}, z_{\tau-1}^{\text{tgt}}, z_{\tau-1}^{\text{har}}$
- 

## 3.3.2 MUTUAL SELF-ATTENTION CONTROL

We diverge from the conventional use of cross-attention mechanisms and instead draw inspiration from the MasaCtrl (Cao et al., 2023) technique to refine music structure through self-attention queries. These queries adeptly navigate through non-rigid musical transformations, aligning with the designated musical theme or instrument (target prompt). The process begins by sketching the foundational musical theme using the target’s self-attention components— $Q^{\text{tgt}}, K^{\text{tgt}}$ , and  $V^{\text{tgt}}$ . This is followed by enriching this theme with elements resembling the thematic content from the source ( $K^{\text{src}}, V^{\text{src}}$ ), steered by  $Q^{\text{tgt}}$ . However, applying this attentive modulation uniformly over all processing layers and through every denoising step might result in a composition excessively mirroring the source. Consequently, echoing the ethos of MasaCtrl, our proposed solution selectively employs mutual self-attention in the decoder portion of our music editing U-Net, initiated after a set number of denoising iterations.

**Scheduling Mutual Self-Attention Control** The application of mutual self-attention is meticulously planned, beginning at a specific denoising step  $S$  and extending beyond a designated layer  $L$ . The strength and influence of this control mechanism are designed as follows:

$$\text{SelfEdit}(Q^{\text{src}}, K^{\text{src}}, V^{\text{src}}, Q^{\text{tgt}}, K^{\text{tgt}}, V^{\text{tgt}}, t) = \begin{cases} Q^{\text{src}}, K^{\text{src}}, V^{\text{src}} & \text{if } t \geq S \text{ and } l \geq L, \\ Q^{\text{tgt}}, K^{\text{src}}, V^{\text{src}} & \text{otherwise} \end{cases} \quad (9)$$

In this framework,  $S$  signifies the denoising step from which the mutual self-attention control commences, serving as a temporal threshold. Similarly,  $L$  distinguishes the layer index below which this nuanced control strategy becomes operational, tailoring the musical output towards the intended artistic direction.

## 3.3.3 HARMONIC BRANCH INTEGRATION

The naive combination of cross-attention control and mutual self-attention control sequentially would lead to sub-optimal results in the original dual-branch setup, especially failing the global attention refinement. To address this issue, we introduce an additional latent harmonic branch, which serves as an intermediate to host the desired composition and structural information in the target music.

Our unified framework is detailed in Algorithm 2. During each forward step of the diffusion process, we start with mutual self-attention control on  $z^{\text{src}}$  and  $z^{\text{tgt}}$  and assign the output to the harmonic branch latent  $z^{\text{har}}$ . This lays the formal structure of the target music. Following this, cross-attention control is applied on  $M^{\text{har}}$  and  $M^{\text{tgt}}$  to refine the semantic information for  $M^{\text{tgt}}$ . As illustrated in Figure 2, the harmonic branch output  $z_0^{\text{har}}$  reflects the requested non-rigid changes (e.g., “violin”), while preserving the rigid content semantics (e.g., “with noise”). The target branch output  $z_0^{\text{tgt}}$  builds upon the structural layout of the  $z^{\text{har}}$  while reflecting the requested rigid changes (e.g., “with noise”).

**Algorithm 2** Disentangled Inversion Technique

---

```

1: Input: A source prompt  $\mathcal{P}$ , a target prompt  $\mathcal{P}^*$ , a source audio latent  $z_0$ , and guidance scale  $\omega$ .
2: Output: A edited audio latent  $z_0^{tgt}$ .
3: Compute the intermediate results  $z_T^*, \dots, z_1^*$  using DDIM inversion over  $z_0$ .
4: Initialize  $z_T^{src} \leftarrow z_T^*$ ,  $z_T^{tgt} \leftarrow z_T^*$ ,  $z_T^{har} \leftarrow z_T^*$ .
5: for  $t = T$  to 1 do
6:    $[\mathbf{d}_{t-1}^{src}, \mathbf{d}_{t-1}^{tgt}, \mathbf{d}_{t-1}^{har}] \leftarrow z_{t-1}^* - \text{DDIM\_Forward}(z_t^{src}, t, [\mathcal{P}, \mathcal{P}^*, \mathcal{P}], \omega)$ 
7:    $z_{t-1}^{src} \leftarrow \text{DDIM\_Forward}(z_t^{src}, t, [\mathcal{P}, \mathcal{P}^*, \mathcal{P}], \omega) + [\mathbf{d}_{t-1}^{src}, \mathbf{0}, \mathbf{0}]$ 
8:    $z_{t-1}^{har} \leftarrow \text{DDIM\_Forward}(z_t^{har}, t, [\mathcal{P}, \mathcal{P}^*, \mathcal{P}], \omega) + [\mathbf{d}_{t-1}^{src}, \mathbf{0}, \mathbf{0}]$ 
9:    $z_{t-1}^{tgt} \leftarrow \text{DDIM\_Forward}(z_t^{tgt}, t, [\mathcal{P}, \mathcal{P}^*, \mathcal{P}], \omega) + [\mathbf{d}_{t-1}^{src}, \mathbf{0}, \mathbf{0}]$ 
10: end for
11: return  $z_0^{tgt}$ 

```

---

## 3.4 DISENTANGLED INVERSION TECHNIQUE

Recognizing the limitations of using DDIM inversion without classifier-free guidance, we observe that it yields an easily modifiable but imprecise approximation of the original audio signal. Increasing the guidance scale enhances editability, but sacrifices reconstruction accuracy due to latent code deviation during editing.

In order to address this issue, our methodology, which we have termed the *Disentangled Inversion Technique* disentangles into three branches: the source, the harmonic, and the target branch. This decoupling is designed to unleash the capabilities of each branch separately. For the source branch, we implement a targeted correction mechanism. By reintegrating the distance  $z_t^* - z_t^{src}$  into  $z_t^{src}$ , we directly mitigate the deviation of the pathway. This straightforward adjustment effectively rectifies the path and minimizes the accumulated errors introduced by both DDIM inversion and classifier-free guidance, thereby enhancing consistency in the reconstructed audio. On the other hand, the target branch and harmonic branch are left unmodified to fully leverage the innate capabilities of diffusion models in generating the desired target audio. The branches’ untouched state ensures that the model’s potential is utilized to its fullest extent, thereby ensuring the fidelity and integrity of the generated audio. We will further discuss this in the Section 4.2.2. The algorithm of Disentangled Inversion Technique has been outlined in Algorithm 2.

Typical diffusion-based editing (Han et al., 2023b; Miyake et al., 2023) involves two parts: an inversion process to get the diffusion space of the audio, and a forward process to perform editing on the diffusion space. Disentangled Inversion can be plug-and-played into the forward process and rectifies the deviation path step by step. Specifically, Disentangled Inversion first computes the difference between  $z_{t-1}^*$  and  $z_{t-1}^{src}$ , then adds the difference back to  $z_{t-1}^{src}$  in DDIM forward. We only add the difference of the source prompt in latent space and update  $z_{t-1}^{src}$ , which is the key to retaining the editability of the target prompt’s latent space.

## 4 EXPERIMENTS

**Implementation Details.** We infer different editing methods using the pre-trained AudioLDM 2 (Liu et al., 2023b) models with 200 inference steps. The setting of baselines is followed by Manor & Michaeli (2024) and is all evaluated on NVIDIA A800 GPU for a fair comparison. We evaluate all methods in ZoMo-Bench across all editing types with fixed length. And we use the MusicDelta subset of the MelodyDB (Bittner et al., 2014) dataset for variable length comparisons, comprised of 34 musical excerpts in varying styles and in lengths ranging from 20 seconds to 5 minutes. Details can be found in Appendix C.

**Evaluation Metrics.** Our models employ a comprehensive evaluation using both objective and subjective metrics to assess essential content preservation, text-audio alignment fidelity, and audio quality. Objective metrics include Structure Distance (SD) (Ju et al., 2023), CLAP (Contrastive Language-Audio Pretraining) Score (Elizalde et al., 2023), LPAPS (Learned Perceptual Audio Patch Similarity) (Iashin & Rahtu, 2021; Paissan et al., 2023), and FAD (Fréchet Audio Distance) (Kilgour et al., 2018). The CLAP Score evaluates how well the edited audio aligns with the target prompt,

Method	Objective Metrics				Subjective Metrics	
	$SD_{\times 10^3} \downarrow$	LPAPS $\downarrow$	FAD $\downarrow$	CLAP Score $\uparrow$	MOS-Q $\uparrow$	MOS-P $\uparrow$
AudioLDM 2	23.86	0.21	10.36	0.58	73.48	70.12
MusicGen	23.39	0.21	6.63	0.59	75.46	71.28
SDEdit	25.87	0.22	12.18	0.40	69.38	66.23
DDIM Inversion	22.52	0.21	9.51	0.49	73.10	3.38
MusicMagus	16.23	0.19	5.15	0.55	75.12	74.34
DDPM-Friendly	18.30	0.19	5.16	0.54	75.27	73.86
<b>MEDIC</b>	<b>11.97</b>	<b>0.15</b>	<b>2.49</b>	<b>0.61</b>	<b>79.81</b>	<b>77.29</b>

Table 1: Comparison with baselines on ZoME-Bench with fixed length about structure, content preservation, and CLAP similarity.

Method	Objective Metrics				Subjective Metrics	
	$SD_{\times 10^3} \downarrow$	LPAPS $\downarrow$	FAD $\downarrow$	CLAP Score $\uparrow$	MOS-Q $\uparrow$	MOS-P $\uparrow$
AudioLDM 2	24.40	0.22	7.07	0.44	66.37	64.28
MusicGen	27.71	0.23	7.70	0.46	67.41	63.76
SDEdit	28.12	0.24	13.21	0.24	62.80	62.18
DDIM Inversion	23.5	0.21	10.12	0.27	65.94	65.73
MusicMagus	25.6	0.22	7.13	0.43	67.45	67.12
DDPM-Friendly	21.53	0.23	6.68	0.30	66.34	67.28
<b>MEDIC</b>	<b>19.5</b>	<b>0.20</b>	<b>6.58</b>	<b>0.51</b>	<b>71.62</b>	<b>70.18</b>

Table 2: Comparison with baselines in variable length setting.

while Structure Distance, LPAPS, and FAD, which have been adapted from image domain metrics, measure the similarity between the edited and source audio. Specifically, LPAPS quantifies the consistency of the edited audio in relation to the source audio, and the FAD metric assesses the distance between two distributions of audio signals. The Structure Distance measures the structural similarity between the edited and source audio. For the subjective evaluation, we conduct crowd-sourced human assessments using the Mean Opinion Score (MOS) to evaluate both editing fidelity (MOS-Q) and content preservation (MOS-P). We attach the details of all metrics in Appendix C.1.

#### 4.1 ZERO-SHOT MUSIC EDITING RESULTS

We present a comparative study of our *Disentangled Inversion Control* (DIC) against several established music generation and editing baselines, including AudioLDM 2 (Liu et al., 2023b), MusicGen (Copet et al., 2023), SDEdit (Liu et al., 2023a), DDIM Inversion Ho et al. (2020), MusicMagus (Zhang et al., 2024), and DDPM-Friendly (Manor & Michaeli, 2024). Utilizing the ZoMo-Bench test set we developed, we assess the quality of the generated audio samples, focusing on two key aspects: Content Preservation and Editing Fidelity. The results, summarized in Table 1, lead to the following conclusions: (1) Our method, MEDIC, significantly outperforms both generation-based and inversion-based models in terms of editing fidelity and audio similarity, demonstrating its effectiveness in addressing complex editing tasks. (2) Although DDPM-Friendly and MusicMagus show improvements in essential content preservation, they struggle to maintain high text-audio alignment compared to generation models. MEDIC effectively addresses accumulated errors, achieving high audio similarity and an impressive CLAP score, reflecting its superior editing fidelity. (3) MEDIC also excels in subjective metrics, achieving the best performance in audio quality and content preservation.

**Variable Length Comparisons** We further evaluate MEDIC against baseline methods in a variable length setting, with the results presented in Table 2. Our analysis leads to the following conclusions: (1) MEDIC outperforms all baselines across all metrics, demonstrating the effectiveness of our approach in variable-length scenarios. (2) Inversion-based baselines experience a significant degradation in CLAP score, while MEDIC maintains the highest CLAP score of 0.51 on the MusicDelta dataset.

**Fine-grained Comparisons on ZoME-Bench** To substantiate the robustness of our method, we delve into fine-grained comparisons across different types of editing. The FAD and CLAP scores are depicted in Figure 3. The insights gleaned from this analysis are as follows: (1) Across all editing



432  
433  
434  
435  
436  
437  
438  
439  
440  
441  
442  
443  
444  
445  
446  
447  
448  
449  
450  
451  
452  
453  
454  
455  
456  
457  
458  
459  
460  
461  
462  
463  
464  
465  
466  
467  
468  
469  
470  
471  
472  
473  
474  
475  
476  
477  
478  
479  
480  
481  
482  
483  
484  
485

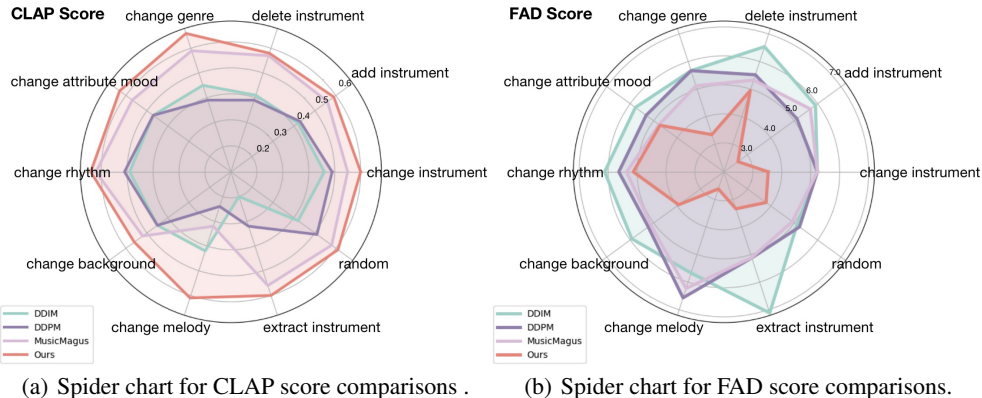


Figure 3: A comprehensive performance evaluation on the ZoME-bench. We present spider charts of CLAP scores and FAD scores across 10 editing tasks for DDPM-Friendly, DDIM Inversion, MusicMagus, and Disentangled Inversion Control methods.

Method	Structure Distance $\times 10^3$ ↓	LPAPS ↓	FAD ↓	CLAP Score ↑
<b>HAC</b>	<b>11.97</b>	<b>0.15</b>	<b>2.49</b>	<b>0.61</b>
w/o MSA Control	14.13	0.19	2.75	0.56
w/o CA Control	13.78	0.18	2.50	0.58
w/o Harmonic Branch	12.75	0.16	2.59	0.59

Table 3: Ablation results about different control methods. MSA: Mutual Self-Attention, CA: Cross Attention.

types, our Disentangled Inversion Control surpasses other methods, demonstrating its prowess in handling both rigid and non-rigid editing tasks. (2) While baselines exhibit capabilities in handling certain rigid editing scenarios, they fall short in executing non-rigid manipulations, as reflected in their inferior performance, especially in the “Change Genre” and “Change Melody” non-rigid editing types.

## 4.2 ABLATION STUDY

The ablation studies presented in this section aim to validate the contributions of the Harmonized Attention Control and Disentangled Inversion to our framework’s overall performance. Additionally, we examine the impact of the classifier-free guidance scale on editing outcomes, with a comprehensive analysis included in Appendix D.

### 4.2.1 ABLATION ON ATTENTION CONTROL METHODS

To validate the impact of our attention control mechanisms, we perform ablations on the following configurations: Remove Mutual Self Attention Control (w/o MSA Control), Remove Cross Attention Control (w/o CA Control), and without Harmonic Branch (w/o Harmonic Branch). The findings, detailed in Table 3, reveal that: (1) Both cross-attention and mutual self-attention controls individually enhance editing performance. (2) Although the naive combination of mutual self-attention control and cross-attention control improves the preservation and fidelity, it still yields sub-optimal outcomes due to the lack of a progressive harmonic branch. This demonstrates the effectiveness of harmonized attention control.

### 4.2.2 ABLATION ON DISENTANGLED INVERSION TECHNIQUE

To demonstrate the soundness of Algorithm 2 and the effective disentanglement of triple branches, we can draw conclusions from Table 4: 1) Incorporating source distance into the target latent and harmonic branch, this leads to a decline in both preservation metrics and CLAP similarity score. 2) Incorporating target distance into the target branch and harmonic branch improves structural

Distance	Structure Distance $\times 10^3 \downarrow$	LPAPS $\downarrow$	FAD $\downarrow$	MSE $\times 10^5 \downarrow$	CLAP Score $\uparrow$
$[d_{src}, d_{src}, \mathbf{0}]$	14.28	0.17	2.64	4.67	0.57
$[d_{src}, \mathbf{0}, d_{src}]$	13.17	0.17	2.55	4.59	0.58
$[d_{src}, d_{tgt}, \mathbf{0}]$	11.24	0.15	2.44	4.32	0.56
$[d_{src}, \mathbf{0}, d_{tgt}]$	<b>11.12</b>	<b>0.14</b>	<b>2.41</b>	<b>4.29</b>	0.56
$[d_{src}, d_{har}, \mathbf{0}]$	37.51	0.27	27.2	14.23	0.28
$[d_{src}, \mathbf{0}, \mathbf{0}]$	11.97	0.15	2.49	4.54	<b>0.61</b>

Table 4: Ablation results from the disentangled inversion technique.  $[\cdot, \cdot, \cdot]$  denotes adding the distance (line 6 in Algorithm 2). MSE means the mean square error loss between the edited audio features and source audio features.

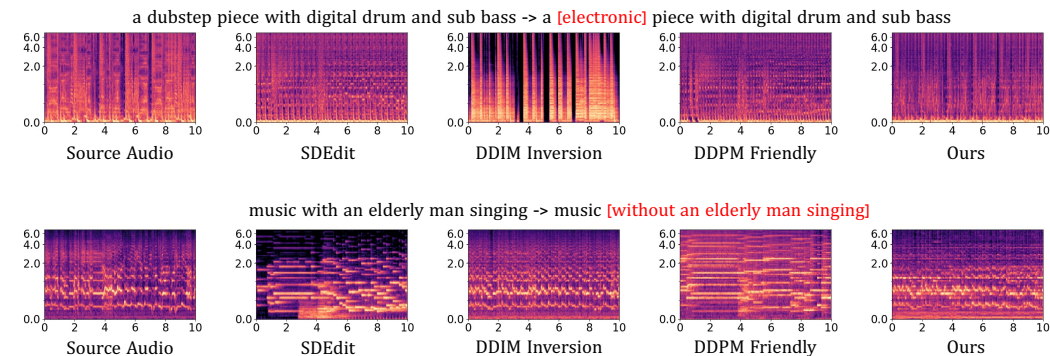


Figure 4: Visualizations of the source audio’s mel and edited mel-spectrograms by different editing methods.

integrity and content preservation. However, this modification leads to a significant decrease in the CLAP score, indicating that while structural quality may improve, the alignment with the target prompt suffers. 3) Adding harmonic distance to the harmonic branch leads to a noticeable decline in performance. This finding showcases that introducing excessive deviations in the harmonic branch may adversely affect the overall audio quality and coherence.

### 4.3 QUALITATIVE RESULTS

To complement our quantitative findings, we present a qualitative comparison in Figure 4. Methods such as SDEdit and inversion-based techniques often struggle to balance high editability with preserving melodic content and harmonic structure. In contrast, our Disentangled Inversion Control performs better in precise music editing while preserving structural integrity. We provide additional qualitative results in the Appendix G for further examination.

## 5 CONCLUSION

In this paper, we explored the burgeoning realm of text-guided diffusion models for audio generation, recognizing their potential to reshape source audio in alignment with specific textual prompts. We proposed the Disentangled Inversion Control to support both rigid and non-rigid editing tasks. Instead of a two-branch setting, we add an intermediate branch named the harmonic branch to progressively integrate harmonic and melodic information in music by cross-attention control and mutual self-attention control. To counteract the accumulated errors caused by DDIM inversion and CFG, we introduced a simple but effective method named disentangled inversion to separate the diffusion process into triple branches and eliminate the latent discrepancy distance in the source branch. Our comprehensive evaluations, conducted on the *ZoME-Bench*—a robust benchmark for music editing comprising 1,100 samples across 10 varied editing categories—attested to the superiority of our methods. And the experiment results on variable length test sets and ablation studies further validated the effectiveness and robustness of our method. We envisage that our work could serve as a basis for future zero-shot music editing studies.

## REFERENCES

- 540  
541  
542 Andrea Agostinelli, Timo I Denk, Zalán Borsos, Jesse Engel, Mauro Verzetti, Antoine Caillon,  
543 Qingqing Huang, Aren Jansen, Adam Roberts, Marco Tagliasacchi, et al. Musiclm: Generating  
544 music from text. *arXiv preprint arXiv:2301.11325*, 2023.
- 545 Rachel M Bittner, Justin Salamon, Mike Tierney, Matthias Mauch, Chris Cannam, and Juan Pablo  
546 Bello. Medleydb: A multitrack dataset for annotation-intensive mir research. In *ISMIR*, volume 14,  
547 pp. 155–160, 2014.
- 548  
549 Tim Brooks, Aleksander Holynski, and Alexei A Efros. Instructpix2pix: Learning to follow image  
550 editing instructions. In *Proceedings of the IEEE/CVF Conference on Computer Vision and Pattern  
551 Recognition*, pp. 18392–18402, 2023.
- 552 Mingdeng Cao, Xintao Wang, Zhongang Qi, Ying Shan, Xiaohu Qie, and Yinqiang Zheng. Masactrl:  
553 Tuning-free mutual self-attention control for consistent image synthesis and editing. In *Proceedings  
554 of the IEEE/CVF International Conference on Computer Vision*, pp. 22560–22570, 2023.
- 555  
556 Ke Chen, Yusong Wu, Haohe Liu, Marianna Nezhurina, Taylor Berg-Kirkpatrick, and Shlomo  
557 Dubnov. Musicldm: Enhancing novelty in text-to-music generation using beat-synchronous mixup  
558 strategies. In *ICASSP 2024-2024 IEEE International Conference on Acoustics, Speech and Signal  
559 Processing (ICASSP)*, pp. 1206–1210. IEEE, 2024.
- 560 Jade Copet, Felix Kreuk, Itai Gat, Tal Remez, David Kant, Gabriel Synnaeve, Yossi Adi, and  
561 Alexandre Défossez. Simple and controllable music generation, 2023.
- 562  
563 Prafulla Dhariwal and Alexander Nichol. Diffusion models beat gans on image synthesis. *Advances  
564 in neural information processing systems*, 34:8780–8794, 2021.
- 565  
566 SeungHeon Doh, Keunwoo Choi, Jongpil Lee, and Juhan Nam. Lp-musiccaps: Llm-based pseudo  
567 music captioning, 2023.
- 568 Wenkai Dong, Song Xue, Xiaoyue Duan, and Shumin Han. Prompt tuning inversion for text-driven  
569 image editing using diffusion models, 2023.
- 570  
571 Alexey Dosovitskiy, Lucas Beyer, Alexander Kolesnikov, Dirk Weissenborn, Xiaohua Zhai, Thomas  
572 Unterthiner, Mostafa Dehghani, Matthias Minderer, Georg Heigold, Sylvain Gelly, et al. An  
573 image is worth 16x16 words: Transformers for image recognition at scale. *arXiv preprint  
574 arXiv:2010.11929*, 2020.
- 575 Benjamin Elizalde, Soham Deshmukh, Mahmoud Al Ismail, and Huaming Wang. Clap learning  
576 audio concepts from natural language supervision. In *ICASSP 2023-2023 IEEE International  
577 Conference on Acoustics, Speech and Signal Processing (ICASSP)*, pp. 1–5. IEEE, 2023.
- 578  
579 Zach Evans, CJ Carr, Josiah Taylor, Scott H Hawley, and Jordi Pons. Fast timing-conditioned latent  
580 audio diffusion. *arXiv preprint arXiv:2402.04825*, 2024a.
- 581  
582 Zach Evans, Julian D Parker, CJ Carr, Zack Zukowski, Josiah Taylor, and Jordi Pons. Long-form  
583 music generation with latent diffusion. *arXiv preprint arXiv:2404.10301*, 2024b.
- 584 Weixi Feng, Xuehai He, Tsu-Jui Fu, Varun Jampani, Arjun Akula, Pradyumna Narayana, Sugato  
585 Basu, Xin Eric Wang, and William Yang Wang. Training-free structured diffusion guidance for  
586 compositional text-to-image synthesis, 2023.
- 587  
588 Bing Han, Junyu Dai, Weituo Hao, Xinyan He, Dong Guo, Jitong Chen, Yuxuan Wang, Yanmin Qian,  
589 and Xuchen Song. Instructme: An instruction guided music edit and remix framework with latent  
590 diffusion models, 2023a.
- 591  
592 Ligong Han, Song Wen, Qi Chen, Zhixing Zhang, Kunpeng Song, Mengwei Ren, Ruijiang Gao,  
593 Anastasis Stathopoulos, Xiaoxiao He, Yuxiao Chen, Di Liu, Qilong Zhangli, Jindong Jiang,  
Zhaoyang Xia, Akash Srivastava, and Dimitris Metaxas. Improving tuning-free real image editing  
with proximal guidance, 2023b.

- 594 Kaiming He, Xiangyu Zhang, Shaoqing Ren, and Jian Sun. Deep residual learning for image  
595 recognition, 2015.
- 596
- 597 Amir Hertz, Ron Mokady, Jay Tenenbaum, Kfir Aberman, Yael Pritch, and Daniel Cohen-Or. Prompt-  
598 to-prompt image editing with cross attention control. *arXiv preprint arXiv:2208.01626*, 2022.
- 599 Jonathan Ho and Tim Salimans. Classifier-free diffusion guidance. In *NeurIPS 2021 workshop on*  
600 *deep generative models and downstream applications*, 2021.
- 601
- 602 Jonathan Ho, Ajay Jain, and Pieter Abbeel. Denoising diffusion probabilistic models. In *Proc. of*  
603 *NeurIPS*, 2020.
- 604 Rongjie Huang, Jiawei Huang, Dongchao Yang, Yi Ren, Luping Liu, Mingze Li, Zhenhui Ye, Jinglin  
605 Liu, Xiang Yin, and Zhou Zhao. Make-an-audio: Text-to-audio generation with prompt-enhanced  
606 diffusion models, 2023.
- 607 Inbar Huberman-Spiegelglas, Vladimir Kulikov, and Tomer Michaeli. An edit friendly ddpn noise  
608 space: Inversion and manipulations, 2024.
- 609
- 610 Vladimir Iashin and Esa Rahtu. Taming visually guided sound generation, 2021.
- 611
- 612 Xuan Ju, Ailing Zeng, Yuxuan Bian, Shaoteng Liu, and Qiang Xu. Direct inversion: Boosting  
613 diffusion-based editing with 3 lines of code. *arXiv preprint arXiv:2310.01506*, 2023.
- 614 Bahjat Kawar, Shiran Zada, Oran Lang, Omer Tov, Huiwen Chang, Tali Dekel, Inbar Mosseri, and  
615 Michal Irani. Imagic: Text-based real image editing with diffusion models. In *Proceedings of the*  
616 *IEEE/CVF Conference on Computer Vision and Pattern Recognition*, pp. 6007–6017, 2023.
- 617
- 618 Kevin Kilgour, Mauricio Zuluaga, Dominik Roblek, and Matthew Sharifi. Fr`echet audio distance:  
619 A metric for evaluating music enhancement algorithms. *arXiv preprint arXiv:1812.08466*, 2018.
- 620 Gwanghyun Kim, Taesung Kwon, and Jong Chul Ye. Diffusionclip: Text-guided diffusion models  
621 for robust image manipulation. In *Proceedings of the IEEE/CVF Conference on Computer Vision*  
622 *and Pattern Recognition*, pp. 2426–2435, 2022.
- 623 Haohe Liu, Zehua Chen, Yi Yuan, Xinhao Mei, Xubo Liu, Danilo Mandic, Wenwu Wang, and  
624 Mark D Plumbley. Audioldm: Text-to-audio generation with latent diffusion models. *arXiv*  
625 *preprint arXiv:2301.12503*, 2023a.
- 626
- 627 Haohe Liu, Qiao Tian, Yi Yuan, Xubo Liu, Xinhao Mei, Qiuqiang Kong, Yuping Wang, Wenwu  
628 Wang, Yuxuan Wang, and Mark D Plumbley. Audioldm 2: Learning holistic audio generation with  
629 self-supervised pretraining. *arXiv preprint arXiv:2308.05734*, 2023b.
- 630 Huadai Liu, Rongjie Huang, Xuan Lin, Wenqiang Xu, Maozong Zheng, Hong Chen, Jinzheng He,  
631 and Zhou Zhao. Vit-tts: visual text-to-speech with scalable diffusion transformer. *arXiv preprint*  
632 *arXiv:2305.12708*, 2023c.
- 633
- 634 Huadai Liu, Rongjie Huang, Yang Liu, Hengyuan Cao, Jialei Wang, Xize Cheng, Siqi Zheng, and  
635 Zhou Zhao. Audioldm: Text-to-audio generation with latent consistency models. *arXiv preprint*  
636 *arXiv:2406.00356*, 2024.
- 637 Hila Manor and Tomer Michaeli. Zero-shot unsupervised and text-based audio editing using ddpn  
638 inversion. *arXiv preprint arXiv:2402.10009*, 2024.
- 639
- 640 Daiki Miyake, Akihiro Iohara, Yu Saito, and Toshiyuki Tanaka. Negative-prompt inversion: Fast  
641 image inversion for editing with text-guided diffusion models, 2023.
- 642 Ron Mokady, Amir Hertz, Kfir Aberman, Yael Pritch, and Daniel Cohen-Or. Null-text inversion for  
643 editing real images using guided diffusion models. In *Proceedings of the IEEE/CVF Conference*  
644 *on Computer Vision and Pattern Recognition*, pp. 6038–6047, 2023.
- 645
- 646 OpenAI. Gpt-4 technical report, 2023.
- 647
- 648 Francesco Paissan, Zhepei Wang, Mirco Ravanelli, Paris Smaragdis, and Cem Subakan. Audio  
649 editing with non-rigid text prompts, 2023.

648 Gaurav Parmar, Krishna Kumar Singh, Richard Zhang, Yijun Li, Jingwan Lu, and Jun-Yan Zhu.  
649 Zero-shot image-to-image translation. In *ACM SIGGRAPH 2023 Conference Proceedings*, pp.  
650 1–11, 2023.

651 William Peebles and Saining Xie. Scalable diffusion models with transformers, 2023.

652

653 Manos Plitsis, Theodoros Kouzelis, Georgios Paraskevopoulos, Vassilis Katsouros, and Yannis  
654 Panagakis. Investigating personalization methods in text to music generation. In *ICASSP 2024-  
655 2024 IEEE International Conference on Acoustics, Speech and Signal Processing (ICASSP)*, pp.  
656 1081–1085. IEEE, 2024.

657

658 Jiaming Song, Chenlin Meng, and Stefano Ermon. Denoising diffusion implicit models. In *Proc. of  
659 ICLR*, 2020.

660

661 Yang Song and Stefano Ermon. Improved techniques for training score-based generative models.  
662 *Advances in neural information processing systems*, 33:12438–12448, 2020.

663

664 Narek Tumanyan, Michal Geyer, Shai Bagon, and Tali Dekel. Plug-and-play diffusion features for  
text-driven image-to-image translation, 2022.

665

666 Ashish Vaswani, Noam Shazeer, Niki Parmar, Jakob Uszkoreit, Llion Jones, Aidan N. Gomez, Lukasz  
Kaiser, and Illia Polosukhin. Attention is all you need, 2023.

667

668 Bram Wallace, Akash Gokul, and Nikhil Naik. Edict: Exact diffusion inversion via coupled transfor-  
669 mations. In *Proceedings of the IEEE/CVF Conference on Computer Vision and Pattern Recognition*,  
670 pp. 22532–22541, 2023.

671

672 Chen Henry Wu and Fernando De la Torre. A latent space of stochastic diffusion models for zero-  
673 shot image editing and guidance. In *Proceedings of the IEEE/CVF International Conference on  
Computer Vision*, pp. 7378–7387, 2023.

674

675 Richard Zhang, Phillip Isola, Alexei A. Efros, Eli Shechtman, and Oliver Wang. The unreasonable  
676 effectiveness of deep features as a perceptual metric, 2018.

677

678 Yixiao Zhang, Yukara Ikemiya, Gus Xia, Naoki Murata, Marco A. Martínez-Ramírez, Wei-Hsiang  
679 Liao, Yuki Mitsufuji, and Simon Dixon. Musicmagus: Zero-shot text-to-music editing via diffusion  
680 models, 2024.

681

682

683

684

685

686

687

688

689

690

691

692

693

694

695

696

697

698

699

700

701

702 A PRELIMINARIES AND ANALYSES

703  
704 This section introduces the foundational concepts of DDIM sampling and classifier-free guidance  
705 as applied to diffusion models for text-guided audio synthesis. It further explores the challenges  
706 associated with these methods.

707  
708 A.1 DIFFUSION MODELS

709  
710 Text-guided diffusion models aim to map a random noise vector  $z_t$  and textual condition  $c$  to an  
711 output audio  $z_0$ , corresponding to the given conditioning prompt. We train a denoiser network  
712  $\epsilon_\theta(z_t, t, c)$  to predict the Gaussian noise  $\epsilon \in \mathcal{N}(0, \mathbf{I})$  following the objective:

713 
$$\min_{\theta} \mathbf{E}_{z_0, \epsilon \in \mathcal{N}(0, \mathbf{I}), t \in \text{Uniform}(1, T)} \|\epsilon - \epsilon_\theta(z_t, t, c)\|^2 \tag{10}$$

714  
715 Where noise is added to the sampled data  $z_0$  according to timestamp  $t$ . At inference, given a noise  
716 vector  $z_T$ , the noise  $i$  is gradually removed by sequentially predicting it using a pre-trained network  
717 for  $T$  steps. To generate audios from given  $z_T$ , we employ the deterministic DDIM sampling:

718 
$$z_{t-1} = \frac{\sqrt{\alpha_{t-1}}}{\sqrt{\alpha_t}} z_t + \sqrt{\alpha_{t-1}} \left( \sqrt{\frac{1}{\alpha_{t-1}} - 1} - \sqrt{\frac{1}{\alpha_t} - 1} \right) \epsilon_\theta(z_t, t, c) \tag{11}$$

721 A.2 DDIM INVERSION

722  
723 While diffusion models have superior characteristics in the feature space that can support various  
724 down-stream tasks, it is hard to apply them to audios in the absence of natural diffusion feature space  
725 for non-generated audios. Thus, a simple inversion technique known as DDIM inversion is commonly  
726 used for unconditional diffusion models, predicated on the presumption that the ODE process can be  
727 reversed in the limit of infinitesimally small steps:

728 
$$z_t^* = \frac{\sqrt{\alpha_t}}{\sqrt{\alpha_{t-1}}} z_{t-1}^* + \sqrt{\alpha_t} \left( \sqrt{\frac{1}{\alpha_t} - 1} - \sqrt{\frac{1}{\alpha_{t-1}} - 1} \right) \epsilon_\theta(z_{t-1}^*, t - 1) \tag{12}$$

730  
731 However, in most text-based diffusion models, this presumption cannot be guaranteed, resulting in a  
732 perturbation from  $z_t$  to  $z_t^*$ . Consequently, an additional perturbation from  $z_t^*$  to  $z_t^{src}$  arises when  
733 sampling an audio from  $z_T^*$  where  $\alpha$  is hyper-parameter:

734 
$$z_t = \sqrt{\alpha_t} z_0 + \sqrt{1 - \alpha_t} \epsilon \tag{13}$$

735  
736 A.3 CLASSIFIER-FREE GUIDANCE

737  
738 Classifier-free Guidance (CFG) (Ho & Salimans, 2021) is proposed to overcome the limitation of  
739 text-conditioned models, where text adherence could be weak. However, a higher guidance scale,  $\omega$ ,  
740 which is intended to strengthen the model’s fidelity to the text prompt, inadvertently magnifies the  
741 accumulated inversion error. This becomes problematic in editing scenarios where precise control  
742 over the audio synthesis is desired. The modified noise estimation in CFG can be expressed as:

743 
$$\hat{\epsilon}_\theta(z_t, t, c, \emptyset) = \omega \cdot \epsilon_\theta(z_t, t, c) + (1 - \omega) \cdot \epsilon_\theta(z_t, t, \emptyset) \tag{14}$$

744 where  $\emptyset = ({}''')$  is the embedding of a null text. This further leads to another perturbation from  $z_t'$  to  
745  $z_t''$  due to the destruction of the DDIM process and causes error augmentation as demonstrated in  
746 Figure 1.

748 B BENCHMARK CONSTRUCTION

749  
750 B.1 GENERAL INFORMATION

751  
752 Here are the details of our ZoME-Bench dataset (Zero-shot Music Editing Benchmark). This dataset  
753 contains 1,000 audio samples, selected from MusicCaps, with each sample being 10 seconds long  
754 and having a sample rate of 16k.

755 We refactor the original captions to express specific edits and divide them into 10 parts, each  
representing a different type of editing. A sample and details are shown in the following table 5.

Editing type id	Editing type	size	origin prompt	editing prompt	editing instruction
0	change instrument	131	ambient acoustic [guitar] music	ambient acoustic [violin] music	change the instrument from guitar to violin
1	add instrument	139	metal audio with a distortion guitar [and drums]	metal audio with a distortion guitar	add drums to the piece
2	delete instrument	133	an eerie tense instrumental featuring electronic drums [and synth keyboard]	an eerie tense instrumental featuring electronic drums	remove the synth keyboard
3	change genre	134	a recording of a solo electric guitar playing [blues] licks	a recording of a solo electric guitar playing [rocks] licks	change the genre from blues to rock
4	change mood	100	a recording featuring electric bass with an [upbeat] vibe	a recording featuring electric bass with an [melancholic] vibe	turn upbeat mood into melancholic mood
5	change rhythm	69	a live ukulele performance featuring [fast] strumming and emotional melodies	a live ukulele performance featuring [slow] strumming and emotional melodies	change fast rhythm into slow one
6	change background	95	female voices in unison with [acoustic] guitar	female voices in unison with [electric] guitar	switch acoustic guitar to electric guitar
7	change melody	121	this instrumental song features a [relaxing] melody	this instrumental song features a [cheerful] melody	change relaxing melody into cheerful melody
8	extract instrument	111	a reggae rhythm recording with bongos [djembe congas acoustic drums and electric guitar]	a reggae rhythm recording with bongos	extract bongos from the recording
9	random	67	/	/	/

Table 5: Information of ZoME-Bench dataset

## B.2 ANNOTATION PROCESS

We rebuild our caption from captions for Musiccaps offered by (Agostinelli et al., 2023). With the help of ChatGPT-4 (OpenAI, 2023), we rebuild the caption with prompt as follows (take type “change melody” as examples):

**Description:** “There is a description of a Piece of music, Please judge whether the description has information of melody. If not, just answer “Flase”, else change its melody properly into the opposite one, just change the adjective and don’t replace any instrument! ”, “blended\_word” is [origin melody,

810 changed melody], “emphasize” is [changed melody], “blended\_word” and “emphasize” are tuples.  
 811 **Question:** (A mellow, passionate melody from a noisy electric guitar)  
 812 **Answer:**(“source\_prompt”: “A mellow, [passionate] melody from a noisy electric guitar”, “edit-  
 813 ing\_prompt”: “A mellow, [soft] melody from a noisy electric guitar”, “blended\_word”: [“passionate  
 814 melody”, “soft melody”], “emphasize”: [“soft melody”])  
 815 **Question:** (A recording of solo harp music with a dreamy, relaxing melody.)  
 816 **Answer:** (“source\_prompt”: “A recording of solo harp music with a dreamy, [relaxing] melody.”, “edit-  
 817 ing\_prompt”: “A recording of solo harp music with a dreamy, [nervous] melody.”, “blended\_word”:  
 818 [“relaxing melody”, “nervous melody”], “emphasize” : [“nervous melody”])  
 819 **Question:** (“A vintage, emotional song with mellow harmonized flute melody and soft wooden  
 820 percussions”)  
 821 **Answer:** (“source\_prompt”: “A vintage, emotional song with [passionate] flute melody and soft  
 822 wooden percussions.”, “editing\_prompt”: “A vintage, emotional song with [harmonized] flute melody  
 823 and soft wooden percussions.”, “blended\_word”: [“harmonized flute melody”, “passionate flute  
 824 melody”]), “emphasize” : [“passionate flute melody”])  
 825 **Now we have Question:**({origin caption}), Answer(?)”

826 In the same way, instructions are appended by prompt as follows (take type “change melody” as  
 827 examples):

828 **Description:** “There are two descriptions of different pieces of music divided by &, Please describe  
 829 the difference you need to give me the results in the following format: Question: this instrumental  
 830 song features a [relaxing] melody with a country feel accompanied by a guitar piano simple percussion  
 831 and bass in a slow tempo & this instrumental song features a [cheerful] melody with a country feel  
 832 accompanied by a guitar piano simple percussion and bass in a slow tempo  
 833 **Answer:** change relaxing melody into cheerful melody  
 834 **Question:** this song features acapella harmonies with a [high pitched] melody complemented by both  
 835 high pitched female whistle tones and male low pitch tones & this song features acapella harmonies  
 836 with a [smooth] melody complemented by both high pitched female whistle tones and male low pitch  
 837 tones  
 838 **Answer:** turn a high pitched melody into smooth melody  
 839 **Question:** a traditional and hopeful song with a harmonizing throaty male vocal and [dissonant]  
 840 background melody from strings albeit presented in low quality & a traditional and hopeful song with  
 841 a harmonizing throaty male vocal and [harmonic] background melody from strings albeit presented  
 842 in low quality  
 842 **Answer:** change dissonant melody into harmonic melody  
 843 **Now we have Question:** [‘source prompt’] & [‘editing prompt’], Answer(?)”

844 Through this method, supplemented by rounds of manual review, we ensure the quality of this  
 845 benchmark.  
 846

### 847 B.3 DATA FORMAT

848 Taking the first piece as an example, we express our data in JSON format with six keys

```
849 {
850   "000000000000": {
851     "editing_prompt": "a live recording of ambient acoustic
852     [violin] music",
853     "source_prompt": "a live recording of ambient acoustic
854     [guitar] music",
855     "blended_word": "(\" guitar \", \" violin \")",
856     "emphasize": "(\" violin \")",
857     "audio_path": "wavs/MusicCaps_-4SYC2YgzL8.wav",
858     "editing_type_id": "0",
859     "editing_instruction": "change the instrument from guitar
860     to violin"
861   }
862 }
863 }
```



“Editing\_prompt” refers to the edited caption, while “source\_prompt” denotes the original caption. “Blended\_word” indicates the subject to be edited, and “Emphasize” represents the word that should be highlighted. “Editing\_instruction” provides a description of the editing process. Additionally, in the editing type “delete instrument,” we introduce another key, “neg\_prompt”, which helps reduce the likelihood of deleted instruments reappearing.

## C IMPLEMENTATION DETAILS

For our evaluation, we utilize the pre-trained AudioLDM 2-Music model (Liu et al., 2023b). Our assessment employs a comprehensive set of metrics, namely CLAP, LPAPS, Structure Distance, and FAD. These metrics are calculated using the CLAP models available in the AudioLDM\_eval package, which is accessible at [https://github.com/haoheliu/audioldm\\_eval](https://github.com/haoheliu/audioldm_eval). In line with the methodology described by Manor & Michaeli (2024), we apply a forward guidance of 3 and a reverse guidance scale of 12 for DDPM inversion. For the DDIM inversion, the guidance scale is set to 5, while for SDEdit, we employ a guidance scale of 12. The forward guidance of MEDIC is 1 while the reverse scale is 5. We chose these values by exploring different guidance scales, as discussed in Appendix D. We conduct all experiments in NVIDIA 4090. For our evaluation, we have selected the public pre-trained AudioLDM 2-Music model (Liu et al., 2023b). To ensure a thorough and multidimensional assessment, we measure performance using a suite of metrics that includes CLAP, LPAPS, Structure Distance, and FAD and conduct on an NVIDIA 4090. The computation of these metrics is facilitated by the CLAP models provided within the AudioLDM\_eval package, which is publicly available at [https://github.com/haoheliu/audioldm\\_eval](https://github.com/haoheliu/audioldm_eval).

Our methodology is aligned with the protocol established by Manor & Michaeli (2024), where we have adopted a forward guidance scale of 3 and a reverse guidance scale of 12 for DDPM inversion. In contrast, the DDIM inversion employs a guidance scale of 5, and SDEdit utilizes a guidance scale of 12. For Disentangled Inversion Control, we have determined the forward guidance to be 1 and the reverse scale to be 5. These specific guidance scale values are selected after extensive experimental exploration, the details of which are discussed in Appendix D.

### C.1 METRICS

**Objective Metrics** There are details about four metrics to evaluate the performance of our novel Disentangled Inversion Control framework: (1) **CLAP Score** (Elizalde et al., 2023): This criterion evaluates the degree to which the output conforms to the specified target prompt. (2) **Structure Distance** (Ju et al., 2023): Leveraging self-similarity of audio features to measure the structure distance between the source and edited audio. (3) **LPAPS** (Iashin & Rahtu, 2021; Paissan et al., 2023): An audio adaptation of the Learned Perceptual Image Patch Similarity (LPIPS) (Zhang et al., 2018), this measure evaluates the consistency of the edited audio with the source audio. (4) **FAD (Fréchet Audio Distance)** (Kilgour et al., 2018): Analogous to the FID used in image analysis, this metric calculates the distance between two distributions of audio signals.

**Subjective Metrics** To directly reflect the quality of the audio generated, we carry out MOS (Mean Opinion Score) tests. These tests involve scoring two aspects: MOS-Q, which assesses the edited quality of the audio, and MOS-P, which measures the content preservation of edited audio.

For assessing editing fidelity, the evaluators were specifically directed to “Does the natural language description align with the audio?” They were provided with both the audio and its corresponding caption. They were then asked to give their subjective rating (MOS-Q) on a 20-100 Likert scale.

To assess essential content preservation, human evaluators were presented with source audio, target audio, source prompt, and target prompt. They were then asked to answer the question, “To what extent does the target audio retain the essential features of the source audio, such as melody, instrumentation, and overall style?” The raters had to select one of the options: “completely,” “mostly,” or “somewhat,” using a 20-100 Likert scale for their response.

Our crowd-sourced subjective evaluation tests were conducted via Amazon Mechanical Turk where participants were paid \$8 hourly.

Guidance Scale		Structure	Background Preservation			CLIP Similarity
Inverse	Forward	Distance $\times 10^3$ ↓	LPAPS ↓	FAD ↓	MSE $\times 10^5$ ↓	CLAP Score ↑
1	1	8.56	0.12	1.17	3.25	0.51
1	2.5	11.97	0.15	2.49	4.54	0.56
1	5	15.99	0.17	4.22	6.07	0.61
1	7.5	15.99	0.17	4.22	6.07	0.59
2.5	1	22.80	0.20	6.39	8.65	0.30
2.5	2.5	14.24	0.16	2.50	5.40	0.46
2.5	5	14.46	0.16	3.31	5.49	0.53
2.5	7.5	15.51	0.17	3.94	5.89	0.53
5	1	29.94	0.24	9.81	11.36	0.20
5	2.5	29.16	0.24	9.11	11.07	0.22
5	5	22.15	0.20	5.59	8.40	0.36
5	7.5	17.57	0.18	5.57	6.67	0.48
7.5	1	31.41	0.25	10.62	11.92	0.20
7.5	2.5	31.05	0.25	10.14	11.78	0.20
7.5	5	29.20	0.24	9.32	11.08	0.24
7.5	7.5	24.16	0.22	7.33	9.17	0.34

Table 6: Ablation Studies on Different Guidance Scale

Method	Inference Time
AudioLDM 2	42.5s
MusicGen	83.3s
SDEdit	44.3s
DDIM Inversion	81.6s
MusicMagus	89.0s
DDPM-Friendly	33.3s
MEDIC	92.0s

Table 7: Inference Time across different methods.

## D QUANTITATIVE RESULTS

**Analyses on Different CFG Scale** The lack of systematic experiments that determine the optimal combination of guidance scales for achieving the best editing performance, and analysis of how these guidance scales affect the final consequence in both reconstruction and editing, we conduct this experiment to find the best scales.

**Inference Time** We compare the inference time of our method with baselines, and the results are compiled in Table 7. MEDIC achieves the comparative inference time with generation models and inversion techniques. We will make an attempt to reduce the inference time of zero-shot music editing in our future work.

## E POTENTIAL NEGATIVE SOCIETAL IMPACTS

MEDIC may also lead to potential negative societal impacts that are worthy of consideration. If the data sample of the training model is not diverse enough or biased, the AI-generated music may be overly biased toward one style or element, limiting the diversity of the music and causing discrimination. MEDIC could be used to create fake audio content, such as faking someone’s voice or creating fake musical compositions, posing the risk of fraud and impersonation. Hopefully, all these issues could be taken into consideration when taking the model for real use to avoid ethical issues.

## F LIMITATIONS

In spite of the remarkable outcome of our method, due to the limitation of the generation model we used, we are incapable of instigating a profound change.

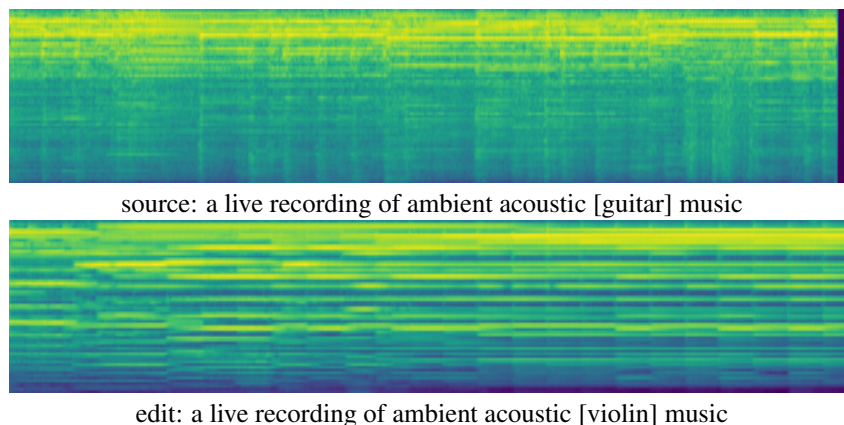
972 Due to the numerous steps it requires ( $T=200$ ), the duration of computing distance is quite long. Thus,  
 973 we will implement a more powerful text-to-music generation model to support better editing, while  
 974 trying to use a consistency model or flow-matching model to achieve high-quality and fast music  
 975 generation in future work. We will make an attempt to edit more interesting and complex music tasks  
 976 in the future.

## 978 G QUALITATIVE RESULTS

979 For each type in ZoME-Bench, We provide samples to observe the capability of MEDIC intuitively.

### 982 G.1 CHANGE INSTRUMENT

984 In Figure 5, we show the capability of MEDIC to change the instrument. Here we edit the ground  
 985 truth music piece with the source prompt “a live recording of ambient acoustic [guitar] music” and  
 986 editing prompt “a live recording of ambient acoustic [violin] music”. The difference in instruments  
 987 can be observed in the Mel-spectrum.



1003 Figure 5: Editing Type 0 :Change Instrument

### 1006 G.2 ADD INSTRUMENT

1008 In Figure 6, we show the capability of MEDIC to add more instruments. Here we edit the ground  
 1009 truth music piece with the source prompt “a heavy metal instructional audio with a distortion guitar”  
 1010 and editing prompt “a heavy metal instructional audio with a distortion guitar [and drums]”. The  
 1011 appearance of the new instrument can be observed in the Mel-spectrum which presents a drum sound  
 1012 of high frequency.

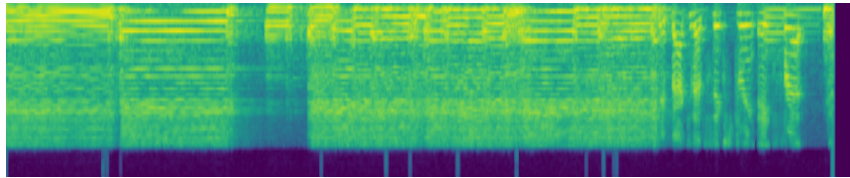
### 1013 G.3 DELETE INSTRUMENT

1015 In Figure 7, we show the capability of MEDIC to delete instruments. Here we edit the ground truth  
 1016 music piece with the source prompt “a lively ska instrumental featuring keyboard trumpets bass  
 1017 [and percussion] with a groovy mood” and the editing prompt “a lively ska instrumental featuring  
 1018 keyboard trumpets and bass with a groovy mood”. The vanishing of the instrument can be observed  
 1019 in the Mel-spectrum.

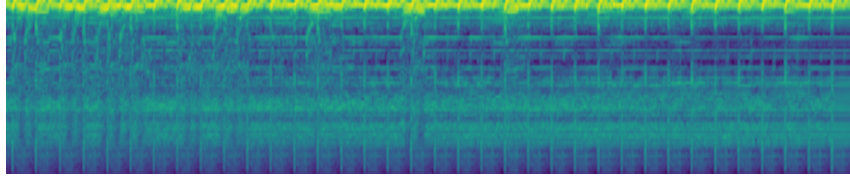
### 1021 G.4 CHANGE GENRE

1023 In Figure 8, we show the capability of MEDIC to change the genre of a music piece. Here we edit the  
 1024 ground truth music piece with the source prompt “a recording of a solo electric guitar playing [blues]  
 1025 licks” and the editing prompt “a recording of a solo electric guitar playing [rock] licks”. The obvious  
 difference in genre can be observed in the Mel-spectrum.

1026  
1027  
1028  
1029  
1030  
1031  
1032  
1033  
1034  
1035  
1036  
1037  
1038  
1039  
1040  
1041  
1042  
1043  
1044  
1045  
1046  
1047  
1048  
1049  
1050  
1051  
1052  
1053  
1054  
1055  
1056  
1057  
1058  
1059  
1060  
1061  
1062  
1063  
1064  
1065  
1066  
1067  
1068  
1069  
1070  
1071  
1072  
1073  
1074  
1075  
1076  
1077  
1078  
1079

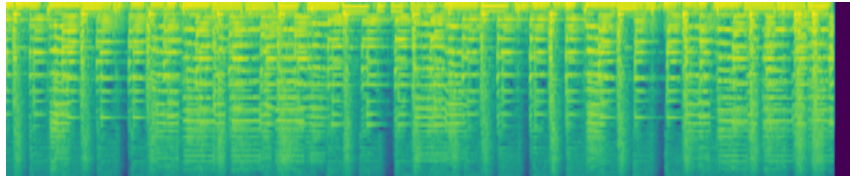


source: a heavy metal instructional audio with a distortion guitar

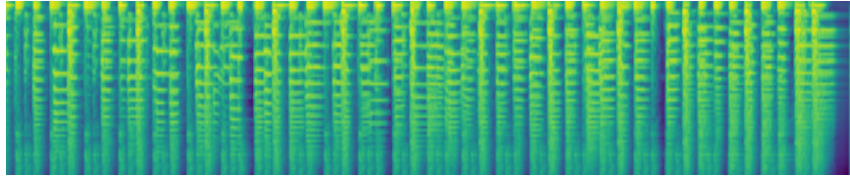


edit: a heavy metal instructional audio with a distortion guitar [and drums]

Figure 6: Editing Type 1 Add Instrument

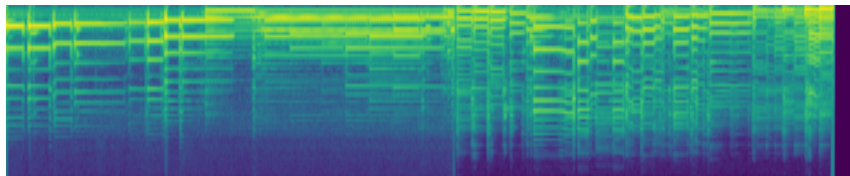


source: a lively ska instrumental featuring keyboard trumpets bass [and percussion] with a groovy mood

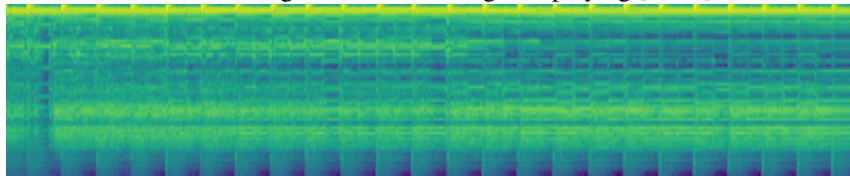


edit: a lively ska instrumental featuring keyboard trumpets and bass with a groovy mood

Figure 7: Editing Type 2 Delete Instrument



source: a recording of a solo electric guitar playing [blues] licks



edit: a recording of a solo electric guitar playing [rock] licks

Figure 8: Editing Type 3 Change Genre

### 1080 G.5 CHANGE MOOD

1081

1082 Mood is an important attribute of music. In Figure 9, we show the capability of MEDIC to change the  
 1083 mood of a music piece. Here we edit the ground truth music piece with the source prompt “a recording  
 1084 of [aggressive] electronic and video game music with synthesizer arrangements” and editing prompt  
 1085 “a recording of [peaceful] electronic and video game music with synthesizer arrangements”. The  
 1086 change of mood can be observed in the Mel-spectrum.

1087

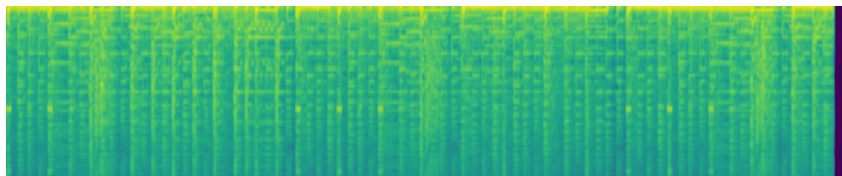
1088

1089

1090

1091

1092



1093 source: a recording of [aggressive] electronic and video game music with synthesizer arrangements

1094

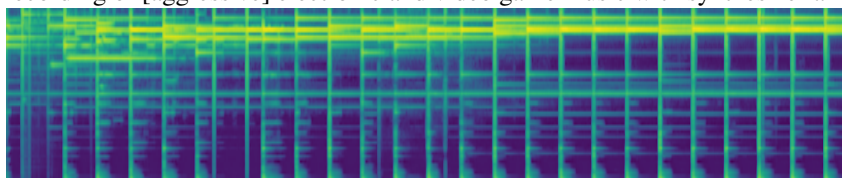
1095

1096

1097

1098

1099



1100 edit: a recording of [peaceful] electronic and video game music with synthesizer arrangements

1101

1102

Figure 9: Editing Type 4 Change Mood

1103

### 1104 G.6 CHANGE RHYTHM

1105

1106 Rhythm represents the speed of the music. In Figure 10, we show the capability of MEDIC to change the  
 1107 Rhythm of a music piece. Here we edit the ground truth music piece with the source prompt “a  
 1108 [slow] tempo ukelele tuning recording with static” and the editing prompt “a [fast] tempo ukelele  
 1109 tuning recording with static”. The change of Rhythm can be observed in the Mel-spectrum. The  
 1110 edited Mel-spectrum is much more intensive.

1111

1112

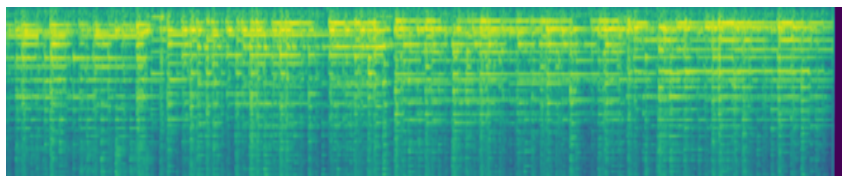
1113

1114

1115

1116

1117



1118 source: a [slow] tempo ukelele tuning recording with static

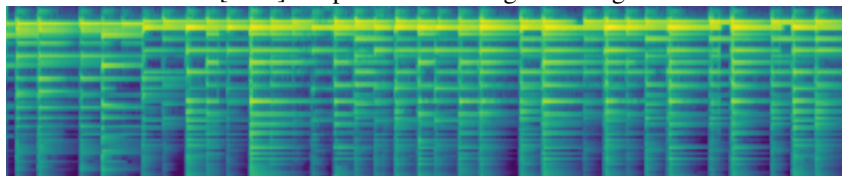
1119

1120

1121

1122

1123



1124 edit: a [fast] tempo ukelele tuning recording with static

1125

1126

1127

1128

1129

1130 In Figure 11, we show the capability of MEDIC to change the background of the instrument of a  
 1131 music piece. Here we edit the ground truth music piece with the source prompt “an amateur ukulele  
 1132 recording with a [medium to uptempo] pace” and editing prompt “an amateur ukulele recording  
 1133 with a [steady and rhythmic] pace”. The change of instrument background can be observed in the  
 Mel-spectrum.

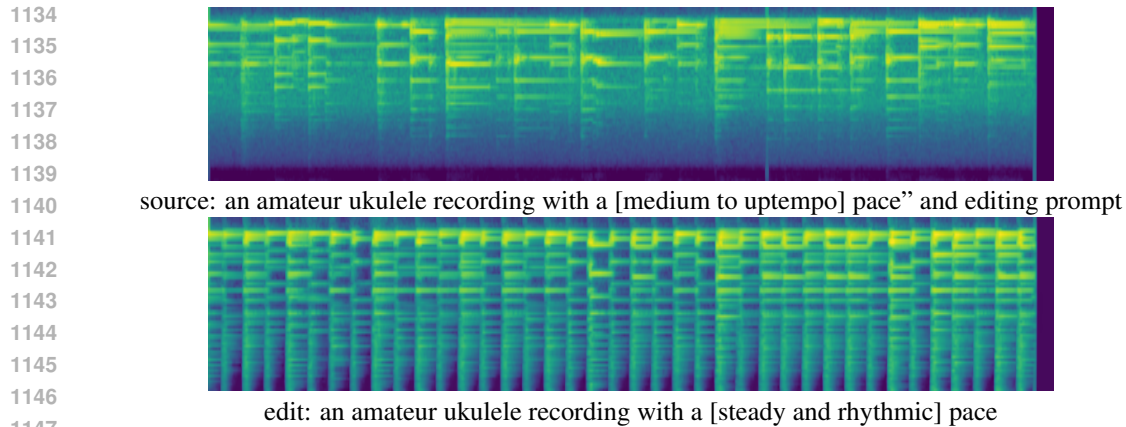


Figure 11: Editing Type 6 Change Background

### 1150 G.8 CHANGE MELODY

1151  
1152 In Figure 12, we show the capability of MEDIC to change the melody of a music piece. Here we edit  
1153 the ground truth music piece with the source prompt “this instrumental song features a [relaxing]  
1154 melody with a country feel accompanied by a guitar piano simple percussion and bass in a slow  
1155 tempo” and editing prompt “this instrumental song features a [cheerful] melody with a country feel  
1156 accompanied by a guitar piano simple percussion and bass in a slow tempo”. The change of Melody  
1157 can be observed in the Mel-spectrum.

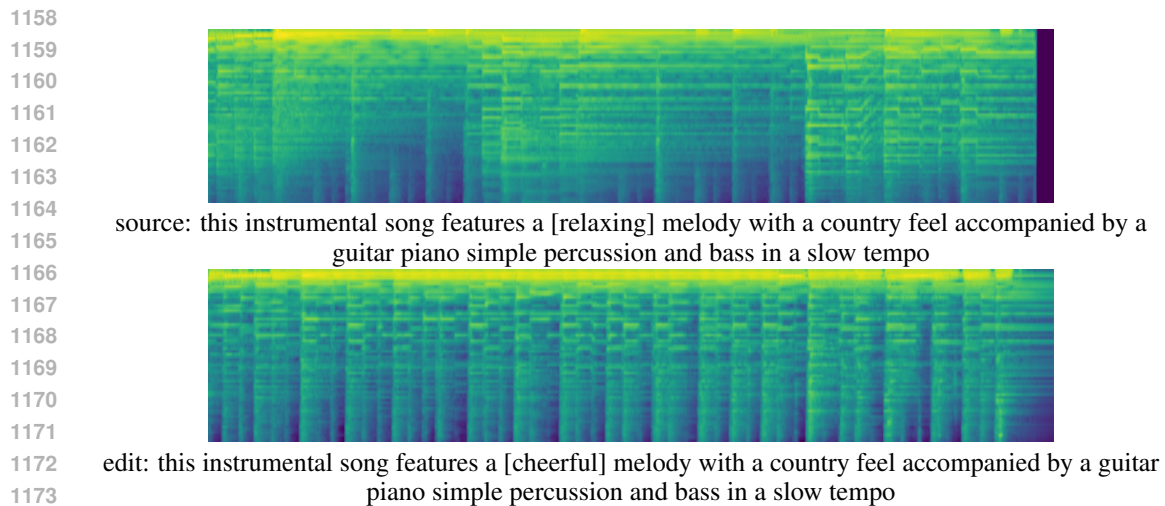


Figure 12: Editing Type 7 Change Melody

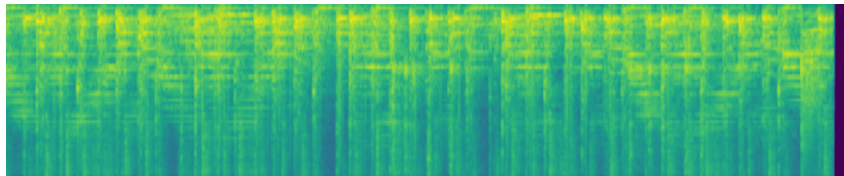
### 1177 G.9 EXTRACT INSTRUMENT

1178  
1179 In Figure 13, we show the capability of MEDIC to extract one certain instrument of a music piece.  
1180 Here we edit the ground truth music piece with the source prompt “a reggae rhythm recording with  
1181 bongos [djembe congas acoustic drums and electric guitar]” and editing prompt “a reggae rhythm  
1182 recording with bongos”. The change of instruments can be observed in the Mel-spectrum.

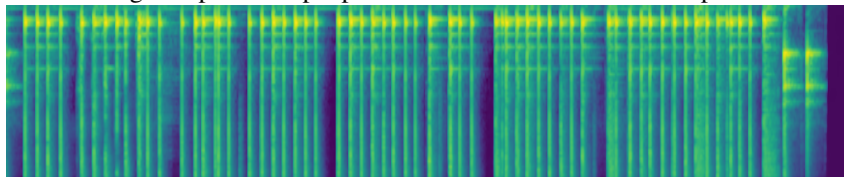
## 1183 H SAFEGUARDS

1184  
1185  
1186 In the processing of the data and models involved in this study, we fully considered the potential  
1187 risks. We ensure that all data sources are rigorously screened and vetted, and the model we used is  
absolutely trained from the safe dataset to minimize the security risks of being misused.

1188  
1189  
1190  
1191  
1192  
1193  
1194  
1195  
1196  
1197  
1198  
1199  
1200  
1201  
1202  
1203  
1204  
1205  
1206  
1207  
1208  
1209  
1210  
1211  
1212  
1213  
1214  
1215  
1216  
1217  
1218  
1219  
1220  
1221  
1222  
1223  
1224  
1225  
1226  
1227  
1228  
1229  
1230  
1231  
1232  
1233  
1234  
1235  
1236  
1237  
1238  
1239  
1240  
1241



source: this instrumental song features a [relaxing] melody with a country feel accompanied by a guitar piano simple percussion and bass in a slow tempo



edit: this instrumental song features a [cheerful] melody with a country feel accompanied by a guitar piano simple percussion and bass in a slow tempo

Figure 13: Editing Type 8 Extract Instrument